

# Luminescent P-Benzyl Dithienophospholes – A Joint Experimental and Theoretical Investigation

Zisu Wang,<sup>A</sup> Alva Y. Y. Woo,<sup>A</sup> and Thomas Baumgartner<sup>A,B</sup>

<sup>A</sup>Department of Chemistry and Centre for Advanced Solar Materials, University of Calgary, 2500 University Drive NW, Calgary, AB, T2N 1N4, Canada.

<sup>B</sup>Corresponding author. Email: thomas.baumgartner@ucalgary.ca

A series of P-benzyl functionalised dithieno[3,2-*b*:2',3'-*b*]phospholes with different substitution pattern at the phosphorus as well as the conjugated scaffold was synthesised and characterised via optical spectroscopy. Single crystal X-ray crystallography was performed on one species. The experimentally observed data were solidified with density functional theory calculations. In contrast to related benzylated P-phenyl phospholium species, the new systems show pronounced photoluminescence in solution, with the exception of the phosphole sulfide species. The observed photophysics could be explained with dominating  $\pi \rightarrow \pi^*$  transitions, despite the presence of the benzyl group that had been found to quench the fluorescence in the predecessor benzyl system with P-phenyl substituent.

Manuscript received: 30 April 2013.

Manuscript accepted: 20 May 2013.

Published online: 26 June 2013.

## Introduction

The development of organic  $\pi$ -conjugated chromophores is an active area of research, as these species have considerable potential for practical applications in very diverse areas, such as organic electronics or the biomedical context.<sup>[1]</sup> The organic nature of the chromophores allows for a relatively efficient way of tuning the electronic properties of the materials at the molecular level, so that they can be employed in organic light-emitting diodes (OLED),<sup>[1a]</sup> organic field-effect transistors (OFET),<sup>[1b]</sup> organic photovoltaics (OPV),<sup>[1c]</sup> but also as sensory materials,<sup>[1d]</sup> photoactive switches,<sup>[1e,f]</sup> and biolabels,<sup>[1f,g]</sup> to name but a few important applications.

However, while generally quite successful, the use of genuine i.e. carbon-based, organic materials does have its limitations, as the modification of the optical and electronic properties of the materials can require laborious synthetic approaches to achieve the desired properties. In order to tailor the materials' properties in a more substantial fashion, the introduction of main group elements into the scaffold of organic  $\pi$ -conjugated materials has recently started to draw an increasing amount of attention. Particularly boron-,<sup>[2]</sup> silicon-,<sup>[3]</sup> and phosphorus-based<sup>[4]</sup> conjugated materials have gained considerable popularity in the field. Due to their intrinsic electronic properties and unique chemistries, these elements have been found to impart very desirable properties onto the carbon-based molecular scaffolds.

Along these lines, we have established the highly luminescent dithieno[3,2-*b*:2',3'-*d*]phosphole system as a powerful chromophore over the past decade (Fig. 1a).<sup>[5]</sup> The phosphorus atom at the core of the molecular scaffold provides a unique set of opportunities for effectively manipulating the photophysical and electronic properties of the system. Through simple modification of a trivalent P-centre (E = lone pair), we were able to significantly change the luminescence properties of the scaffold, but we could also show that incorporation of the P-centre

generally introduces considerable electron-acceptor character.<sup>[4e,5d,6]</sup> Both features are made possible – as a result of the strongly pyramidal nature of the phosphorus – through an orbital interaction between the  $\sigma^*$ -orbital of the exocyclic P-substituent(s) and the  $\pi^*$ -system of the main scaffold (Fig. 1b).

In the context of designing dithienophosphole-based self-organising materials, we were recently able to access the novel phosphole-lipid system (Fig. 1c) that can form smectic liquid-crystal (LC) phases (A),<sup>[7]</sup> or one-dimensional fibrous organogels (B)<sup>[8]</sup> from hydrocarbon solvents, depending on the nature of the conjugated scaffold. Next to the self-assembly behaviour,

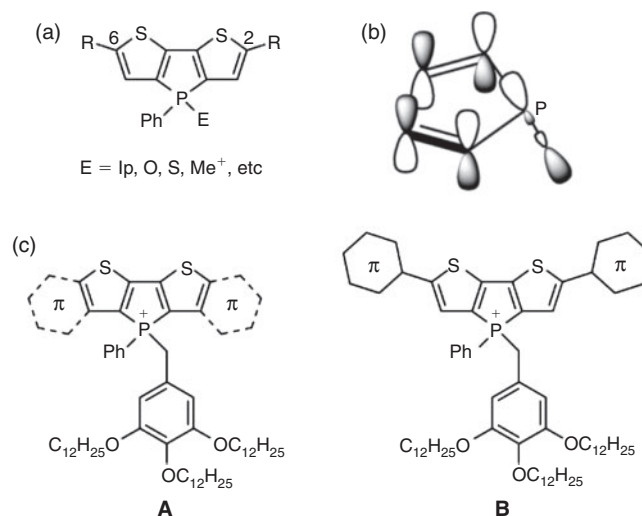


**Fig. 1.** (a) Dithienophosphole system (lp = lone pair); (b)  $\sigma^*$ - $\pi^*$ -interaction in phospholes; (c) liquid-crystalline (A) and organogel-forming (B) phosphole-lipids.

the LC-forming species **A** also showed some unexpected photo-physical properties. In contrast to simple dithienophospholes, these benzylated phospholium species do not exhibit pronounced luminescence in solution at room temperature, but they rather show aggregation-induced enhanced emission behaviour in the solid state. Through extensive studies, involving a series of suitable model compounds,<sup>[9]</sup> we could establish that the benzyl group at the phosphorus centre provides several non-radiative relaxation pathways that quench the luminescence in solution, which are based on i) the inherent flexibility of this substituent leading to intramolecular rotation, and ii) its electronic nature that opens up photoinduced electron-transfer (PET) processes, particularly for electron-rich benzyl groups.

To further elaborate the effects of a benzyl substituent at the phosphorus centre on the overall photophysics of dithienophospholes, we now report the structure-property study of a new family of species that exhibit an exocyclic benzyl substituent instead of the common phenyl group at phosphorus. This allowed us to investigate the effects of further functionalisation of the P-centre using simple modifications according to our established protocols. It should be noted that due to the benzylation being the last functionalisation step in the original phosphole-lipids,<sup>[7,9]</sup> these modifications are not possible with the earlier system. In this study, we have further addressed the flexibility of the system by investigating two scaffold variations with and without steric bulk that should have an impact on potential intramolecular rotation. Our experimental studies involving detailed optical investigations have also been supported by extensive theoretical calculations.

## Results and Discussion

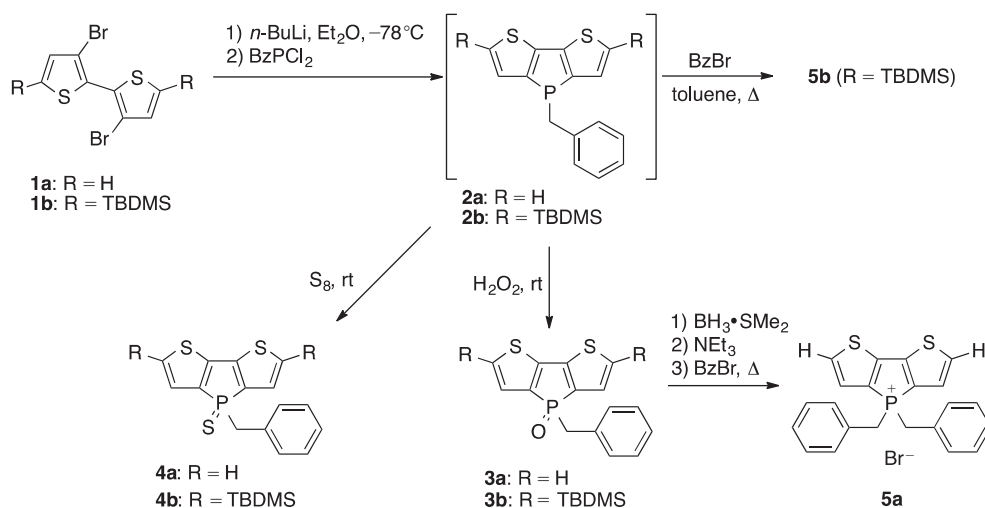
### Synthesis

In order to potentially control and limit the degree of rotational freedom of the benzyl substituent we have targeted two scaffold variations: one that has no substituents at the 2- and 6-position of the scaffold, and another that exhibits bulky *t*-BuMe<sub>2</sub>Si (TBDMS) substituents at these positions. The synthesis of the corresponding 3,3'-dibromo-bithiophene precursors **1a,b** followed reported procedures<sup>[5b,10]</sup> and the incorporation of the phosphorus centre was adapted from the known synthesis towards the P-phenyl substituted dithienophospholes<sup>[5]</sup> using benzyl dichlorophosphate (BzPCl<sub>2</sub>) instead of PhPCl<sub>2</sub> in Et<sub>2</sub>O at -78°C after lithiation of **1a,b** with *n*-BuLi (Scheme 1).

Unfortunately, the isolation of the trivalent species **2a** and **2b** posed some unexpected difficulties, particularly in case of the oily **2a** that precluded its isolation in pure form, whereas **2b** could be recrystallised. In the case of **2a**, oxidation of the crude product and subsequent reduction according to our established two-step protocol using BH<sub>3</sub>•SMe<sub>2</sub> and NEt<sub>3</sub><sup>[11]</sup> provided a means of purification. However, both **2a** and **2b** could ultimately not be purified to full satisfaction. The identity of both species, on the other hand, could nevertheless be established via multinuclear NMR spectroscopy.

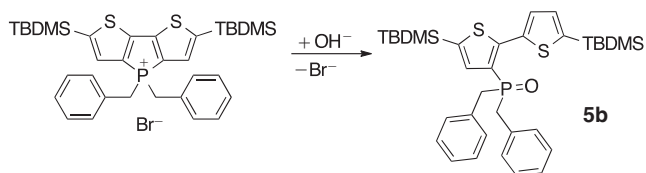
Consequently, we opted to oxidise the crude **2a,b** according to our established protocols using H<sub>2</sub>O<sub>2</sub> to provide the corresponding oxides **3a** and **3b**, which could then be isolated in appreciable purity in moderate to low yields (**3a**: 26%; **3b**: 38%).<sup>[5]</sup> The same applies to the corresponding phosphole sulfides that were obtained in 20% (**4a**) and 48% (**4b**) after treatment with elemental sulfur and column chromatography, respectively.<sup>[5b]</sup> To complete the series, we also targeted the bis(benzyl)phospholium species **5a,b** to provide a suitable link between the new and the original benzylated systems. In terms of synthesis, **5a** was generated via reduction of the phosphole oxide **3a**, following our reported two-step procedure,<sup>[11]</sup> and subsequent treatment with benzyl bromide, providing **5a** in moderate yield (36%). For the synthesis of the silylated species, the crude trivalent phosphole **2b** was treated with benzyl bromide, which allowed for the isolation of **5b** in 37% using preparative TLC.

Multinuclear NMR spectroscopy revealed some interesting features that provided valuable insights into the molecular structures of the new species. The 2,6-H-terminated species **3a–5a**, showed highly symmetric sets of signals for the organic scaffold, with <sup>31</sup>P NMR shifts of δ 26.4 ppm for **3a**, 31.3 ppm for **4a**, and 25.3 ppm for **5a** and a single <sup>1</sup>H/<sup>13</sup>C NMR signal for the benzyl CH<sub>2</sub>-group in form of a typical doublet due to coupling with phosphorus, suggesting no specific interaction of the benzyl group with the conjugated scaffold in solution. Notably, the <sup>31</sup>P resonances are downfield-shifted from the values for the available P-phenyl congeners (PO: 19.0 ppm;<sup>[5a]</sup> PBz<sup>+</sup>: 18.8 ppm<sup>[7]</sup>), likely as a result of the different electronics of the benzyl group, but they show a similarly small split between them. The TBDMS-substituted species **3b** and **4b** also showed comparable features to those observed for related P-phenyl congeners as well as **3a** and **4a**, with <sup>31</sup>P NMR shifts of



Scheme 1. Synthesis of the benzylated dithienophospholes.

$\delta$  25.1 ppm for **3b** and 28.9 ppm for **4b** (c.f.: PO: 14.9 ppm; PS(SiMe<sub>3</sub>)<sub>2</sub>: 23.6 ppm).<sup>[5b]</sup> In line with earlier observations on TBDMS-substituted dithienophospholes, the SiMe<sub>2</sub> resonances are split into two signals, due to the restricted rotation resulting from the bulky nature of the *t*-Bu group. X-ray crystal structure analyses of several related P-phenyl dithienophospholes have revealed an *anti* arrangement of these groups with one *t*-Bu group residing above and the other below the planar  $\pi$ -conjugated scaffold.<sup>[5b,12]</sup> From these NMR data, a similar conformation can thus also be assumed for the new species. The bis(benzylated) species **5b**, however, showed some distinctly different NMR data from those of the other relatives. Its <sup>31</sup>P NMR shift of  $\delta$  32.8 ppm is clearly downfield-shifted from those of the corresponding oxide and sulfide congeners, opposite to the H-terminated series. In addition, the *t*-Bu and Me resonances of the TBDMS group are split into two different sets of signals in 1 : 1 ratios with a much more pronounced split between them ( $\Delta\delta(^1\text{H}) = 0.1$  ppm for both *t*-Bu and Me) suggesting different environments for each of the two groups. Furthermore, the benzyl CH<sub>2</sub>-group shows a higher-order splitting pattern in the <sup>1</sup>H NMR spectrum, which clearly deviates from the doublet seen for the other relatives (see Supplementary



**Scheme 2.** Ring-opening reaction in the presence of OH<sup>−</sup> leading to **5b**.

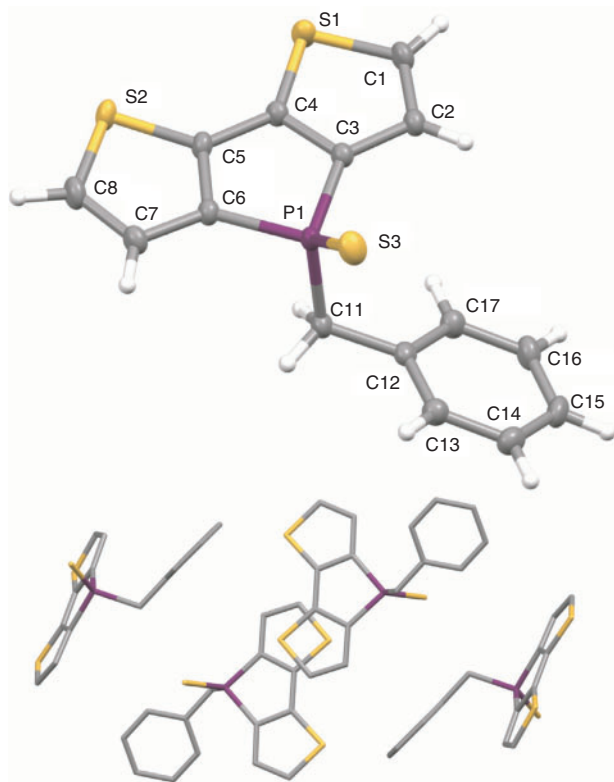


**Fig. 2.** Molecular structure of **4a** (top, 50% probability level) and intermolecular interaction (bottom) in the solid state. Selected bond lengths (Å): C1–C2: 1.361(2); C2–C3: 1.416(2); C3–C4: 1.378(2); C4–C5: 1.456(2); C5–C6: 1.374(2); C6–C7: 1.412(2); C7–C8: 1.362(2); P1–C3A: 1.8064(15); P1–C6: 1.8027(14); P1–C31: 1.8277(16); P1–S3: 1.9436(5).

Material). A distinctly different molecular structure is further suggested by the presence of 11 aromatic resonance signals in the <sup>13</sup>C NMR spectrum (as opposed to the expected eight signals seen in the aromatic region for the other congeners). The 1D- as well as 2D-NMR data for **5b** thus clearly support an unsymmetrical molecular scaffold as a result of the ring-opened phosphole unit. It is well known that phosphole systems (including dithienophospholes) tend to ring-open in the presence of alkoxides or hydroxides.<sup>[13]</sup> HRMS data confirms the absence of the bromide anion that has been formally exchanged for OH<sup>−</sup>. Consequently, OH<sup>−</sup> (likely from water) must have been present during the synthesis of **5b**, whose steric congestion further enabled the ring-opening process leading to the product shown in **Scheme 2**.

We were able to obtain single crystals of **4a** by slow diffusion of pentane into an acetone solution at room temperature, that were suitable for an X-ray diffraction study (**Fig. 2**, **Table 1**). The bond lengths and angles of the main scaffold are completely in line with those of other crystallographically characterised dithienophospholes, suggesting excellent  $\pi$ -conjugation.<sup>[5–7,11,12]</sup> Compared with a related P-phenyl species, the exocyclic P1–C11 is slightly elongated at 1.8277(16) Å (c.f.: 1.810(3) Å),<sup>[5b]</sup> which can be attributed to the sp<sup>3</sup>-hybridised nature of the benzyl CH<sub>2</sub>-group. The P1–S3 bond length of 1.9436(5) Å is also slightly elongated with respect to the P-phenyl congener (c.f.: 1.9267(13) Å).<sup>[5b]</sup> The most pronounced structural feature is the fact that the benzyl group does not reside above the  $\pi$ -conjugated scaffold, but is rotated away from it. This is surprising, since all of the originally reported benzylated P-phenyl dithienophospholes exhibit the former conformation.<sup>[7,9]</sup> However, intermolecular packing involving the benzyl group that could lead to the observed conformation could not be discerned from the X-ray crystallography; the only ‘strong’ intermolecular interaction arises from partial  $\pi$ – $\pi$  stacking of the conjugated scaffold.

#### Photophysical Properties

To our surprise, almost all of the new P-benzyl species **3–5** turned out to be highly fluorescent in solution and the solid state.

**Table 1.** Crystal data and refinement details for **4a**

Temperature [K]	173(2)
Formula	C <sub>15</sub> H <sub>11</sub> PS <sub>3</sub>
Formula weight	318.42
Crystal system	Monoclinic
Space group	P21/n
<i>a</i> [Å]	10.59110(10)
<i>b</i> [Å]	6.4870(10)
<i>c</i> [Å]	21.9877(2)
$\alpha$ [°]	90
$\beta$ [°]	94.0391(2)
$\gamma$ [°]	90
<i>V</i> [Å <sup>3</sup> ]	1445.15(3)
<i>Z</i>	4
<i>F</i> <sub>000</sub>	656
<i>D</i> <sub>calc</sub> [g cm <sup>−3</sup> ]	1.464
R <sub>int</sub> col/ind	26451/2838
<i>R</i> <sub>(int)/Prms</sub>	0.0290/216
<i>R</i> <sub>1</sub> [ <i>I</i> > 2σ( <i>I</i> )]	0.0290
<i>wR</i> <sub>2</sub> [ <i>I</i> > 2σ( <i>I</i> )]	0.0775
GoF	1.093
Peak/Hole	0.494/−0.198

As exception, the phosphole sulfides **4a,b** are only weakly fluorescent. Given the fact that both the oxides **3a,b** as well as the bis(benzyl)phospholium species **5a,b** are indeed highly fluorescent, the weak luminescence of **4a,b** could likely be attributed to the heavy atom effect of the sulfur, rather than intramolecular rotation. A similar feature was observed in the recently reported dithiazolophosphole system.<sup>[14]</sup> The photophysical data of **3a,b–5a,b** are summarised in Table 2 and the UV/Vis spectra are shown in Fig. 3.

In line with our earlier observations on the P-phenyl congeners,<sup>[5b]</sup> the absorption and emission wavelengths of the phosphole oxide and sulfide species are nearly identical (**3a**:  $\lambda_{\text{abs}} = 356$  nm;  $\lambda_{\text{em}} = 437$  nm, **4a**:  $\lambda_{\text{abs}} = 357$  nm;  $\lambda_{\text{em}} = 444$  nm). In addition, the TBDMS groups lead to a small red shift in absorption of **3b** and **4b**, as well as increased extinction coefficients, that are also similar to earlier observations and can be attributed to the  $\sigma$ -donor/ $\pi$ -acceptor character of this substituent (**3b**:  $\lambda_{\text{abs}} = 369$  nm; **4b**:  $\lambda_{\text{abs}} = 369$  nm), while the emission of **4b** does not show a similar shift ( $\lambda_{\text{em}} = 443$  nm; c.f. **3b**:  $\lambda_{\text{em}} = 444$  nm). Moreover, there is a distinct difference in the photoluminescence quantum yields of the oxide and sulfide species, respectively (**3a,b**  $\phi_{\text{PL}} \approx 69\%$ ; **4a,b**  $\phi_{\text{PL}} \approx 1\%$ ). It is also worth mentioning that while the bis(benzyl) species **5a** shows a similar behaviour as related P-phenyl phospholium species with further red-shifted absorption and emission wavelengths ( $\lambda_{\text{abs}} = 366$  nm;  $\lambda_{\text{em}} = 452$  nm),<sup>[7,9]</sup> the absorption and emission wavelengths of **5b** are blue-shifted to all the other species in this series ( $\lambda_{\text{abs}} = 305$  nm;  $\lambda_{\text{em}} = 406$  nm); this

**Table 2.** Photophysical properties of compounds **3a,b**, **4a,b**, and **5a,b** in solution

Compound	$\lambda_{\text{abs}}^{\text{A}}$ [nm]	$\epsilon$ [ $\text{L mol}^{-1} \text{cm}^{-1}$ ]	$\lambda_{\text{em}}^{\text{A}}$ [nm]	$\phi_{\text{PL}}^{\text{B}}$
<b>3a</b>	356	7370	437	69 %
<b>3b</b>	369	12100	444	69 %
<b>4a</b>	310, 357	5910, 6600	444	0.7 %
<b>4b</b>	315, 369	5970, 13100	443	1.6 %
<b>5a</b>	366	5450	452	16 %
<b>5b</b>	305	10500	406	99 %

<sup>A</sup>In dichloromethane,  $c \approx 10^{-6}$  M.

<sup>B</sup>Versus aqueous quinine sulfate 0.1 M.

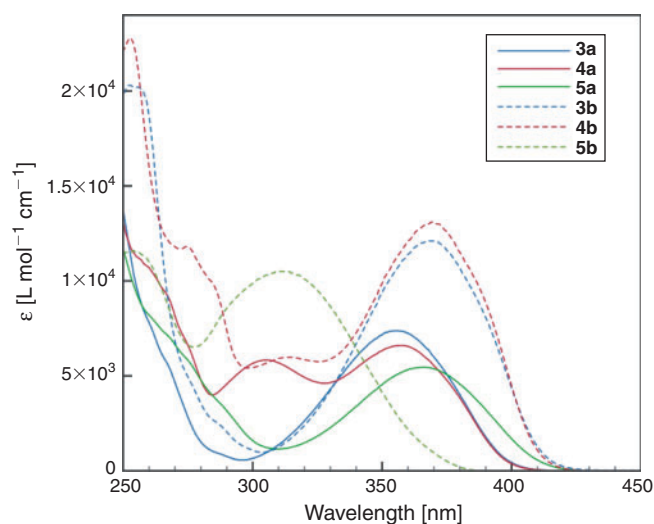


**Fig. 3.** UV-Vis spectra of the P-benzyl dithienophospholes in dichloromethane.

deviation reflects the observed NMR data and confirms the disruption of the conjugation due to ring-opening (see above).<sup>[13b]</sup> The photoluminescence quantum yields of **5a** and **5b** are also quite different with  $\phi_{\text{PL}} = 0.16$  for **5a**, and an impressive value near unity for **5b**, which is likely the result of a very rigid molecular scaffold in **5b** due to steric congestion.

### Theoretical Calculations

To gain some deeper insight into the observed experimental features, we have optimised the molecular structures of compounds **2a–5a** (as well as the originally targeted ring-closed **5b'**) using density functional theory (DFT) calculations at the B3LYP/6–31+G(d) level of theory<sup>[15]</sup> that has provided satisfactory results for the dithienophosphole system before.<sup>[5–7,11]</sup> In all cases, the minimisation resulted in a molecular structure similar to that observed with **4a** in the solid state. As can be seen in Fig. 4, the benzyl group is rotated away from the conjugated scaffold, the latter of which also dominates the frontier orbitals. Similar to typical dithienophospholes, the HOMO represents the  $\pi$ -system, whereas the LUMO represents the  $\pi^*$ -system with the phosphole-typical  $\sigma^*-\pi^*$  interaction.<sup>[5]</sup> Depending on the P-functionalisation, the  $\pi$ -system of the benzyl group is part of the HOMO-1. However, in most cases, the HOMO-1 energies are significantly lower than those of the corresponding HOMO, which indicates only a remote possibility for these orbitals to be involved in optical transitions. It is consequently plausible that the optical transitions are dominated by  $\pi \rightarrow \pi^*$  transitions leading to the observed strong photoluminescence of the system (see below). The calculations further confirm that the sulfur lone pairs of **4a** are indeed involved in the optical transitions (as part of the HOMO, but also the HOMO-1, which is nearly degenerate to the HOMO as a result of the heavy atom effect) and clearly explain the quenched fluorescence of **4a**. The second, high-energy absorption band at  $\lambda_{\text{abs}} = 310$  nm in the UV spectra of **4a** (Fig. 3), which is absent for the other species (except **4b**), also supports this conclusion.

In order to verify that the conformation of the benzyl group does not have a considerable impact in the photophysics (other than the previously established shift in absorption and emission),<sup>[7,9]</sup> we have also calculated rotational conformers of **2a**, **3a**, and **5a**, in which the benzyl group resides above the conjugated scaffold. It should be noted that, when the benzyl group was placed above the scaffold as input, the optimisation also provided a local energy minimum with this conformation. However, no discernable energy difference between the two conformers could be detected, suggesting that while free rotation of the benzyl group should be possible, it does not lead to noticeable differences in the optical transitions. In fact, most of the orbital distributions, as well as energies remain fairly close to those of the corresponding 'anti'-conformers (Fig. 5).

The calculations for the ring-closed **5b'** (polarisable continuum model, PCM; solvation,  $\text{CH}_2\text{Cl}_2$ ) suggest a conformation similar to that of **5a-rot** (see Supplementary Material) with electron-density distributions and energies close to those obtained for the frontier orbitals of the non-silylated species **5a-rot**. The only difference is the  $\sigma$ -donor/ $\pi$ -acceptor character of the TBDMS group, which is reflected in slightly different energies for **5b'** (HOMO-1:  $E = -7.34$  eV; HOMO:  $E = -6.58$  eV; LUMO:  $E = -2.94$  eV). This further indirectly supports the ring-opened nature of the experimentally isolated **5b**.

To finally verify the nature of the observed optical transitions, we have also performed time-dependent (TD)-DFT calculations using both rotational isomers of **3a** as well as *anti*-**4a**

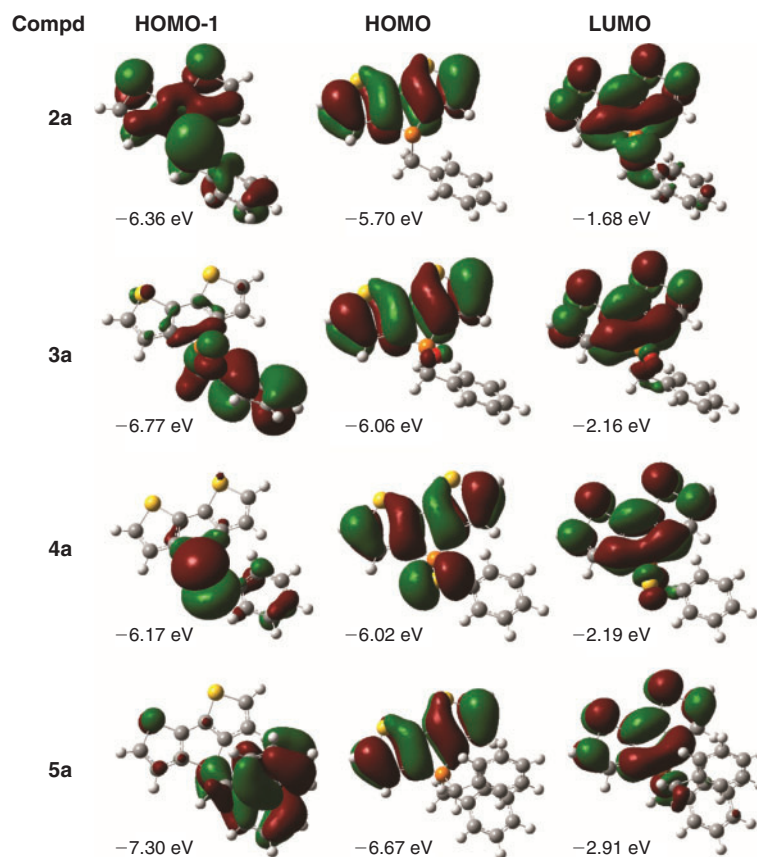


Fig. 4. DFT-calculated orbitals (HOMO-1, HOMO, and LUMO) and energies of minimised structures of **2a–5a** in *anti*-conformation. A PCM solvation model ( $\text{CH}_2\text{Cl}_2$ ) was applied to **5a** to account for the omission of the counter anion.

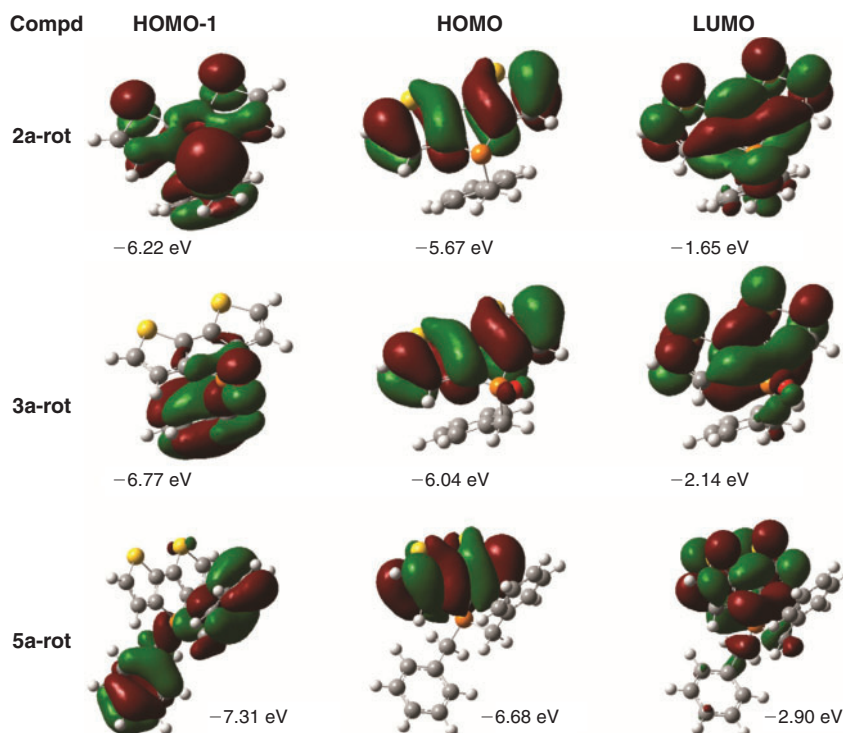


Fig. 5. DFT-calculated orbitals (HOMO-1, HOMO, and LUMO) and energies of minimised structures of **2a-rot**, **3a-rot**, and **5a-rot** in *syn*-conformation. A PCM solvation model ( $\text{CH}_2\text{Cl}_2$ ) was applied to **5a-rot** to account for the omission of the counter anion.

as representative examples. For both isomers of **3a**, the lowest-energy absorption, which also happens to be the most intense (as derived from its oscillator strength), corresponds to HOMO → LUMO (100%; **3a**:  $f=0.1677$ , **3a-rot**:  $f=0.1533$ ), with the absorption wavelength showing a slight shift as a function of the conformation (**3a**: 360 nm; **3a-rot**: 362 nm), in line with our earlier observations and the optical spectroscopy data. By contrast, the most intense absorption for **4a** at 342 nm ( $f=0.1681$ ) is a combination of HOMO-2 → LUMO (73.2%) and HOMO → LUMO (11.7%). The HOMO-2 ( $E = -6.35$  eV) has a similar distribution to that of the HOMO, however with a bonding combination between the sulfur lone pair and the  $\pi$ -system of the scaffold. The TD-DFT data thus clearly support that the observed optical spectroscopy data indeed involve strong  $\pi$ - $\pi^*$  transitions, regardless of the conformation and consequently explain the significant photoluminescence of the new system. Moreover, the mixing of the sulfur lone pair with the  $\pi$ - $\pi^*$  transitions also explains the origin of the reduced luminescence of **4a**. The calculations further eliminate the possibility of PET and thus explain the distinctly different behaviour of this system compared with the originally reported P-phenyl benzyl-phospholium species.

## Conclusion

We have synthesised two sets of dithienophospholes with P-benzyl groups that were functionalised with either hydrogen or TBDMS groups at the 2,6-positions of the molecular scaffold. Utilising standard phosphorus-modification protocols, we have further modified this centre with a variety of substituents including oxygen, sulfur, and benzyl. The 2,6-H-terminated phosphole sulfide could be characterised crystallographically. Its structure showed a conformation in which the benzyl group was rotated away from the conjugated scaffold, in contrast to the P-phenyl relatives. Moreover, most of the new species unexpectedly showed pronounced photoluminescence in solution, with the exception of the phosphole sulfides, which is also in contrast to the P-phenyl relatives and the result of dominant  $\pi \rightarrow \pi^*$  transitions. Due to steric congestion and the resulting ring-opening of the central phosphole unit, the TBDMS-terminated bis(benzylated) relative of this series showed unexpected blue-shifted photophysics, however, with an impressive quantum yield near unity that is distinctly different from the other relative in this series.

The experimental data could be corroborated by TD-DFT calculations at the B3LYP/6-31+G(d) level of theory that suggest that while the benzyl group is indeed somewhat flexible in the present system, intramolecular rotation does not affect its pronounced luminescence in solution. The same is true for photo-induced electron transfer that can be excluded to occur from the calculations. This deviating behaviour to the original phosphole-lipids can thus be explained with the different electronics of the benzyl group (compared with phenyl), which seems to make non-radiative relaxation pathways energetically unfavourable. Future investigations will include the substitution of the benzyl group with moieties that exhibit stronger electron-donating character to further elucidate the boundaries of this group's effect on the photophysics of the scaffold.

## Experimental

### General

All chemical reagents were purchased from commercial sources (Aldrich, Alfa Aesar) and were, unless otherwise noted, used without further purification. Solvents were dried using an

MBraun solvent purification system before use. 3,3'-Dibromo-2,2'-bithiophene (**1a**),<sup>[10]</sup> and 5,5'-bis(*t*-butyldimethylsilyl)-3,3'-dibromo-2,2'-bithiophene (**1b**)<sup>[5b]</sup> were prepared according to reported procedures. All reactions and manipulations were carried out under a dry nitrogen atmosphere employing standard Schlenk techniques. <sup>1</sup>H, <sup>13</sup>C, and <sup>31</sup>P NMR were recorded in CDCl<sub>3</sub> on Bruker DRX400 and Avance (-II,-III) 400 MHz spectrometers. Chemical shifts were referenced to external 85% H<sub>3</sub>PO<sub>4</sub> (<sup>31</sup>P) or residual non-deuterated solvent peaks (<sup>1</sup>H, <sup>13</sup>C). Mass spectra were run on a Finnigan SSQ 7000 spectrometer or a Bruker Daltonics AutoFlex III system. All photophysical experiments were carried out on a Jasco FP-6600 spectrofluorometer and UV-Vis-NIR Cary 5000 spectrophotometer. Quantum yields were referenced to aqueous quinine sulfate in 0.1 M sulfuric acid (excitation at 366 nm;  $\phi_{\text{PL}} = 0.54$ ). Theoretical calculations have been carried out at the B3LYP/6-31+G(d) level by using the GAUSSIAN 03 suite of programs using a PCM solvation model (solvent = CH<sub>2</sub>Cl<sub>2</sub>) for the benzylated species.<sup>[14]</sup>

### Crystal Structure Determination and Refinement

A single crystal of **4a** was mounted on MiTeGen micro-loops and then placed under an Oxford Cryosystems Cryostream Plus for temperature control. The crystal structure determination was carried out on a Bruker APEX II diffractometer with graphite-monochromated CuK <sub>$\alpha$</sub>  radiation (1.5418 Å) at 173 K. The intensity data collection was performed in the  $\omega$ - $\phi$  scanning mode with the goniometer and detector angular settings optimised. The unit cells and the orientation matrices were refined using the entire dataset of reflections. The diffraction spots were measured in full, scaled with S<sub>A</sub>I<sub>N</sub>T, corrected for Lorentz-polarisation correction, and integrated using S<sub>A</sub>I<sub>N</sub>T (Bruker).<sup>[16]</sup> All structures were solved using direct methods with SHELXS-97 software and least-squares refinement against  $F^2$  was performed with SHELXL-97 software.<sup>[17]</sup> Anisotropic temperature factors were used for refinement of all atoms excluding hydrogen; hydrogen atoms were refined using isotropic temperature factors in the riding mode. All crystal structure figures were created using Mercury 3 software. CCDC-935961 contains the supplementary crystallographic data for compound **4a**. These data can be obtained free of charge from The Cambridge Crystallographic Data Centre via [www.ccdc.cam.ac.uk/data\\_request/cif](http://www.ccdc.cam.ac.uk/data_request/cif).

### Synthetic Procedures

#### P-Benzyl-dithieno[3,2-b:2',3'-d]phosphole Oxide (**3a**)

3,3'-Dibromo-2,2'-bithiophene (2.01 g, 6.2 mmol) was dissolved in 250 mL dry Et<sub>2</sub>O. The solution was cooled to  $-78^\circ\text{C}$ . *n*-Butyllithium (2.5 M in Et<sub>2</sub>O, 5.1 mL, 12.75 mmol) was added dropwise at  $-78^\circ\text{C}$ . The reaction was kept at this temperature for 1.5 h. Dichlorobenzylphosphine (1.2 g, 6.2 mmol) was dissolved in 15 mL of Et<sub>2</sub>O then added slowly to the reaction at  $-78^\circ\text{C}$ . After the addition, the suspension was warmed up to room temperature with a water bath. Solvent was removed under vacuum. The residue was taken up in pentane then filtered through a neutral alumina plug. Pentane was then replaced with 40 mL of CH<sub>2</sub>Cl<sub>2</sub>. H<sub>2</sub>O<sub>2</sub> (6 mL) was added and the reaction was stirred overnight. The solution was dried by MgSO<sub>4</sub> then concentrated. Column chromatography (CH<sub>2</sub>Cl<sub>2</sub> : MeCN = 10 : 1) afforded the product as an off-white solid (0.48 g, 26%).  $\lambda_{\text{max}}/\text{nm}(\epsilon/\text{M}^{-1}\text{cm}^{-1})$  356 (7370);  $\delta_{\text{H}}$  (CDCl<sub>3</sub>) 7.28–7.19 (m, 5H, Ph), 7.13–7.06 (m, 2H, thieno), 7.04 (dd, <sup>1</sup> $J_{\text{H-H}} = 4.8$  Hz, <sup>3</sup> $J_{\text{H-P}} = 2.1$  Hz, 2H, thieno), 3.48 (d, <sup>2</sup> $J_{\text{H-P}} = 15.5$  Hz, 2H,

P-CH<sub>2</sub>-Ph);  $\delta_P$  -27.49;  $\delta_C$  145.28 (d,  $J_{C-P}$  = 23.0 Hz), 137.03 (d,  $J_{C-P}$  = 107.1 Hz), 131.29 (d,  $J_{C-P}$  = 8.4 Hz), 129.66 (d,  $J_{C-P}$  = 5.6 Hz), 128.40 (d,  $J_{C-P}$  = 3.2 Hz), 127.83 (d,  $J_{C-P}$  = 14.4 Hz), 127.06 (d,  $J$  = 3.7 Hz), 126.22 (d,  $J_{C-P}$  = 13.7 Hz), 37.77 (d,  $J_{C-P}$  = 67.6 Hz);  $m/z$  (HR-MS ESI) 303.0065; [M+H]<sup>+</sup> requires 303.0062.

P-Benzyl-dithieno[3,2-b:2',3'-d]phosphole Sulfide (**4a**)

3,3'-Dibromo-2,2'-bithiophene (0.32 g, 1 mmol) was dissolved in 50 mL dry Et<sub>2</sub>O. The solution was cooled to -78°C. *n*-Butyllithium (2.5M in Et<sub>2</sub>O, 0.8 mL, 2 mmol) was added dropwise at -78°C. The reaction was kept at this temperature for 1.5 h. Dichlorobenzylphosphine (0.19 g, 1 mmol) was dissolved in 5 mL of Et<sub>2</sub>O then added slowly to the reaction at -78°C. After the addition, the suspension was warmed up with a room temperature water bath. Solvent was removed under vacuum. The residue was taken up in pentane then filtered through a neutral alumina plug. Pentane was then replaced with 10 mL of CH<sub>2</sub>Cl<sub>2</sub>. S<sub>8</sub> powder (0.13 g, 4 mmol) was added. The reaction was stirred overnight, after which the solution was concentrated. Column chromatography (CH<sub>2</sub>Cl<sub>2</sub>:hexane = 1:1) afforded the product as a light yellow powder (0.065 g, 20%).  $\lambda_{\max}/\text{nm}(\epsilon/\text{M}^{-1}\text{cm}^{-1})$  357 (6600);  $\delta_H$  7.24 (dd,  $^3J_{H-H}$  = 4.7 Hz,  $^2J_{H-P}$  = 3.8 Hz, 2H, Ph), 7.13 (m, 3H, Ph), 7.07 (dd,  $^1J_{H-H}$  = 4.9 Hz,  $^3J_{H-P}$  = 2.0 Hz, 2H, thieno), 6.93–6.85 (m, 2H, thieno), 3.57 (d,  $^2J_{H-P}$  = 14.7 Hz, 2H, P-CH<sub>2</sub>-Ph);  $\delta_P$  32.35;  $\delta_C$  144.03 (d,  $J_{C-P}$  = 18.9 Hz), 139.65 (s), 138.77 (s), 131.05 (d,  $J_{C-P}$  = 9.2 Hz), 129.66 (d,  $J_{C-P}$  = 5.8 Hz), 128.09 (d,  $J_{C-P}$  = 10.0 Hz), 127.27 (d,  $J_{C-P}$  = 4.3 Hz), 125.66 (d,  $J_{C-P}$  = 14.8 Hz), 42.92 (d,  $J_{C-P}$  = 49.0 Hz).  $m/z$  (HR-MS ESI) 318.9831; [M+H]<sup>+</sup> requires 318.9834.

P-Benzyl-dithieno[3,2-b:2',3'-d]phosphole (**2a**)

P-Benzyl-dithieno[3,2-b:2',3'-d]phosphole oxide **3a** (0.3 g, 1 mmol) was dissolved in 20 mL CH<sub>2</sub>Cl<sub>2</sub>. BH<sub>3</sub>•SMe<sub>2</sub> (2 M in Et<sub>2</sub>O, 2.5 mL, 5 mmol) was added. The reaction was stirred for 3 h at room temperature. All volatile material was removed under vacuum. 20 mL CH<sub>2</sub>Cl<sub>2</sub> was used to dissolve the residue, NEt (1 mL, 7.1 mmol) was added. The reaction was stirred at room temperature for 3 h. All volatile material was removed under vacuum. The residue was washed several times with pentane and then dissolved in CH<sub>2</sub>Cl<sub>2</sub>. The solution was passed through a neutral alumina plug. Evaporation of solvent under vacuum afforded the crude product as a thick yellow oil (0.2 g, 70%).  $\delta_H$  7.48–7.11 (m, 5H, Ph), 7.02 (m, 4H, thieno), 3.15 (s, 2H, P-CH<sub>2</sub>-Ph);  $\delta_P$  -21.04;  $\delta_C$  146.77 (d,  $J_{C-P}$  = 13.4 Hz), 136.79 (d,  $J_{C-P}$  = 1.9 Hz), 128.98 (d,  $J_{C-P}$  = 5.1 Hz), 128.30 (d,  $J_{C-P}$  = 1.3 Hz), 127.08 (d,  $J_{C-P}$  = 18.4 Hz), 126.34 (d,  $J_{C-P}$  = 2.5 Hz), 125.83 (d,  $J_{C-P}$  = 5.7 Hz), 124.30 (d,  $J_{C-P}$  = 59.0 Hz), 35.56 (d,  $J_{C-P}$  = 19.4 Hz);  $m/z$  (HR-MS ESI) 286.0035; [M]<sup>+</sup> requires 286.0040.

P,P-Dibenzyl-dithieno[3,2-b:2',3'-d]phospholium Bromide (**5a**)

P-Benzyl-dithieno[3,2-b:2',3'-d]phosphole oxide (0.49 g, 1.6 mmol) was dissolved in 50 mL CH<sub>2</sub>Cl<sub>2</sub>. BH<sub>3</sub>•SMe<sub>2</sub> (2 M in Et<sub>2</sub>O, 4.1 mL, 8.2 mmol) was added. The reaction was stirred at room temperature for 3 h. All volatile materials were then pumped off. The residue was dissolved in CH<sub>2</sub>Cl<sub>2</sub>. NEt<sub>3</sub> (1.2 mL, 8.6 mmol) was added. The reaction was again stirred at room temperature for 3 h. All volatile materials were, again pumped off. Toluene (30 mL) and THF (15 mL) were used to dissolve the residue. Benzylbromide (0.5 g, 2.9 mmol) was added. The reaction was heated and stirred overnight at reflux.

Afterwards, a bright yellow precipitate had formed and was filtered off. The crude product was washed with acetone then crystallised from a mixture of methanol and acetone to afford the product as light yellow crystals (0.4 g, 36%).  $\lambda_{\max}/\text{nm}(\epsilon/\text{M}^{-1}\text{cm}^{-1})$  366 (5450);  $\delta_H$  8.04 (dd,  $^1J_{H-H}$  = 5.0 Hz,  $^3J_{H-P}$  = 1.7 Hz, 2H, thieno), 7.43 (dd,  $^3J_{H-H}$  = 5.0,  $^2J_{H-P}$  = 4.0 Hz, 2H, thieno), 7.23 – 7.16 (m, 4H, Ph), 7.16–7.04 (m, 6H, Ph), 5.03 (d,  $^2J_{H-P}$  = 15.7 Hz, 4H, P-CH<sub>2</sub>-Ph);  $\delta_P$  26.35;  $\delta_C$  149.66 (d,  $J_{C-P}$  = 17.0 Hz), 130.11 (d,  $J_{C-P}$  = 5.9 Hz), 129.87 (d,  $J_{C-P}$  = 13.6 Hz), 129.73 (d,  $J_{C-P}$  = 14.0 Hz), 128.82 (d,  $J_{C-P}$  = 3.8 Hz), 128.43 (d,  $J_{C-P}$  = 4.4 Hz), 127.39 (d,  $J_{C-P}$  = 9.9 Hz), 125.43 (d,  $J_{C-P}$  = 93.5 Hz), 29.21 (d,  $J_{C-P}$  = 41.2 Hz);  $m/z$  (HR-MS ESI) 377.0583; [M-Br]<sup>+</sup> requires 377.0583.

P-Benzyl-2,6-bis(*tert*-butyldimethylsilyl)-dithieno[3,2-b:2',3'-d]phosphole (**2b**)

3,3'-Dibromo-5,5'-bis(*tert*-butyldimethylsilyl)-2,2'-bithiophene (1.6 g, 2.9 mmol) and N,N,N',N'-tetramethylethylenediamine (2.25 mL, 15 mmol) were dissolved in 72 mL Et<sub>2</sub>O. The solution was cooled to -78°C. *n*-Butyllithium (2.5 M in Et<sub>2</sub>O, 2.3 mL, 5.75 mmol) was added dropwise to the solution. The reaction was kept at this temperature for 1 h. Dichlorobenzylphosphine (0.56 g, 2.9 mmol) was dissolved in 15 mL of Et<sub>2</sub>O then added to the reaction slowly. After the addition, the reaction was warmed up with a warm water bath. Subsequently, the solvent was removed under vacuum. The residue was taken up in pentane then filtered through a neutral alumina plug. The product was obtained as a beige amorphous powder (0.56 g, 22%).

$\delta_H$  7.09–7.08 (m, 3H, Ph), 7.03 (s, 2H, thieno), 6.88–6.83 (m, 2H, Ph), 3.10 (d,  $^2J_{H-P}$  = 3.5 Hz, 2H, P-CH<sub>2</sub>-Ph) 0.92 (s, 18H, *t*Bu-Si), 0.28 (d,  $J_{H-P}$  = 1.2 Hz, 12H, *Me*-Si);  $\delta_P$  -24.78;  $\delta_C$  148.69 (d,  $J_{C-P}$  = 14.3 Hz), 147.65 (s), 139.15 (d,  $J_{C-P}$  = 3.7 Hz), 136.57 (s), 134.79 (d,  $J_{C-P}$  = 17.1 Hz), 128.87 (d,  $J_{C-P}$  = 4.6 Hz), 128.00 (d,  $J_{C-P}$  = 1.7 Hz), 126.07 (d,  $J_{C-P}$  = 2.5 Hz), 35.62 (d,  $J_{C-P}$  = 19.7 Hz), 26.52 (s), 17.15 (s), -4.77 (d,  $J_{C-P}$  = 2.7 Hz);  $m/z$  (HR-MS EI) 514.1764; [M]<sup>+</sup> requires 514.1769.

P-Benzyl-2,6-bis(*tert*-butyldimethylsilyl)-dithieno[3,2-b:2',3'-d]phosphole Oxide (**3b**)

P-Benzyl-2,6-bis(*tert*-butyldimethylsilyl)-dithieno[3,2-b:2',3'-d]phosphole (0.09 g, 0.17 mmol) was dissolved in 10 mL CH<sub>2</sub>Cl<sub>2</sub>. H<sub>2</sub>O<sub>2</sub> (30% solution, 1 mL) was added. The reaction was stirred in open air overnight. TLC (CH<sub>2</sub>Cl<sub>2</sub>:MeCN = 5:1) afforded the product as a white solid (0.035 g, 38%).  $\lambda_{\max}/\text{nm}(\epsilon/\text{M}^{-1}\text{cm}^{-1})$  369 (12100);  $\delta_H$  7.20–7.14 (m, 3H, Ph), 7.07 (d,  $^3J_{H-P}$  = 1.8 Hz, 2H, thieno), 7.02 (m, 2H, Ph), 3.46 (d,  $^2J_{H-P}$  = 15.6 Hz, 2H, P-CH<sub>2</sub>-Ph), 0.93 (s, 18H, *t*Bu-Si), 0.28 (s, 12H, *Me*-Si);  $\delta_P$  26.12;  $\delta_C$  150.21 (d,  $J_{C-P}$  = 23.6 Hz), 142.08 (d,  $J_{C-P}$  = 10.5 Hz), 138.86 (d,  $J_{C-P}$  = 103.9 Hz), 133.59 (d,  $J_{C-P}$  = 12.4 Hz), 131.58 (d,  $J_{C-P}$  = 8.4 Hz), 129.70 (d,  $J_{C-P}$  = 5.5 Hz), 128.28 (d,  $J_{C-P}$  = 3.2 Hz), 126.95 (d,  $J_{C-P}$  = 3.7 Hz), 37.92 (d,  $J_{C-P}$  = 66.8 Hz), 26.23 (s), 16.88 (s), -5.04 (d,  $J_{C-P}$  = 3.1 Hz);  $m/z$  (HR-MS ESI) 531.1783; [M+H]<sup>+</sup> requires 531.1792.

P-Benzyl-2,6-bis(*tert*-butyldimethylsilyl)-dithieno[3,2-b:2',3'-d]phosphole Sulfide (**4b**)

P-Benzyl-2,6-bis(*tert*-butyldimethylsilyl)-dithieno[3,2-b:2',3'-d]phosphole (0.105 g, 0.20 mmol) was dissolved in 5 mL CH<sub>2</sub>Cl<sub>2</sub>. S<sub>8</sub> powder (0.013 g, 0.4 mmol) was added. The reaction was stirred overnight. Preparative TLC (CH<sub>2</sub>Cl<sub>2</sub>:hexane = 1:1) afforded the product as a yellow solid (0.053 g, 48%).  $\lambda_{\max}/\text{nm}(\epsilon/\text{M}^{-1}\text{cm}^{-1})$  369 (13100);  $\delta_H$  7.21 (d,  $J$  = 1.9 Hz, 2H,

thieno), 7.18–7.14 (m, 1H, *p*-Ph), 7.13–7.06 (m, 2H, Ph), 6.91–6.83 (m, 2H, Ph), 3.63 (d,  $^2J_{H-P}$  = 14.7 Hz, 2H, *P-CH<sub>2</sub>-Ph*), 0.97 (d,  $J$  = 2.9 Hz, 18H, *tBu-Si*), 0.33 (d,  $J$  = 5.1 Hz, 12H, *Me-Si*);  $\delta_p$  29.89;  $\delta_C$  149.01 (d,  $J_{C-P}$  = 19.6 Hz), 142.41 (d,  $J_{C-P}$  = 10.7 Hz), 140.70 (d,  $J_{C-P}$  = 86.0 Hz), 132.94 (d,  $J_{C-P}$  = 13.4 Hz), 131.28 (d,  $J_{C-P}$  = 9.2 Hz), 129.62 (d,  $J_{C-P}$  = 5.7 Hz), 127.87 (d,  $J_{C-P}$  = 3.8 Hz), 127.13 (d,  $J_{C-P}$  = 4.3 Hz), 43.34 (d,  $J_{C-P}$  = 48.5 Hz), 26.28 (s), 16.90 (s), -4.99 (d,  $J_{C-P}$  = 3.9 Hz);  $m/z$  (HR-MS ESI) 547.1558;  $[M+H]^+$  requires 547.1563.

*P,P*-Dibenzyl-3-(5,5'-bis(*t*-butyldimethylsilyl)-2,2'-dithienyl) Phosphane Oxide (**5b**)

*P*-Benzyl-2,6-bis(*tert*-butyldimethylsilyl)-dithieno[3,2-*b*:2',3'-*d*]phosphole (0.101 g, 0.2 mmol) was dissolved in 4 mL toluene and 2 mL THF before addition of benzylbromide (0.045 g, 0.20 mmol). The reaction was stirred overnight at reflux. After work-up, preparative TLC (CH<sub>2</sub>Cl<sub>2</sub>:MeCN = 1:1) afforded the product as a white solid (0.05 g, 37%).  $\lambda_{max}/nm(\epsilon/M^{-1} cm^{-1})$  305 (10300);  $\delta_H$  7.54 (d,  $^2J_{H-P}$  = 3.4 Hz, 1H, thieno), 7.27–7.19 (m, 6H, Ph), 7.16 (d,  $^2J_{H-P}$  = 3.1 Hz, 1H, thieno), 7.12 (m, 4H, Ph), 3.24 (dt,  $J_{H-H}$  = 36.1,  $^2J_{H-P}$  = 14.5 Hz, 4H, *P-CH<sub>2</sub>-Ph*), 0.98 (s, 9H, *tBu-Si*), 0.87 (s, 9H, *tBu-Si*), 0.36 (s, 6H, *Me-Si*), 0.24 (s, 6H, *Me-Si*);  $\delta_p$  32.84;  $\delta_C$  147.62 (d,  $J_{C-P}$  = 12.1 Hz), 140.70 (s), 139.70 (d,  $J_{C-P}$  = 12.0 Hz), 139.09 (s), 138.36 (d,  $J_{C-P}$  = 10.6 Hz), 135.87 (s), 131.78 (d,  $J_{C-P}$  = 7.4 Hz), 131.09 (s), 129.97 (d,  $J_{C-P}$  = 5.3 Hz), 128.48 (d,  $J_{C-P}$  = 1.9 Hz), 126.78 (d,  $J_{C-P}$  = 2.4 Hz), 37.27 (d,  $J_{C-P}$  = 65.4 Hz), 26.30 (d,  $J_{C-P}$  = 10.4 Hz), 16.82 (d,  $J_{C-P}$  = 12.8 Hz), -4.99 (d,  $J_{C-P}$  = 14.0 Hz);  $m/z$  (HR-MS CI) 622.2356;  $[M]^+$  requires 622.2345.

### Supplementary Material

Fluorescence spectra of **3a,b**–**5a,b**, frontier orbitals for **5b'**, and final coordinates of DFT-calculated species, as well as copies of the NMR spectra of **2a,b**–**5a,b** are available on the Journal's website.

### Acknowledgements

Financial support by NSERC of Canada and the Canada Foundation for Innovation (CFI) is gratefully acknowledged. Z.W. thanks Alberta Innovates – Technology Futures for a graduate scholarship, and A.Y.Y.W. the University of Calgary for a Queen Elizabeth (II) graduate scholarship.

### References

- [1] (a) *Organic Light Emitting Diodes* (Eds K. Müllen, U. Scherf) **2005** (Wiley-VCH: Weinheim).  
(b) J. E. Anthony, *Angew. Chem. Int. Ed.* **2008**, *47*, 452. doi:10.1002/ANIE.200604045  
(c) A. Mishra, P. Bäuerle, *Angew. Chem. Int. Ed.* **2012**, *51*, 2020. doi:10.1002/ANIE.201102326  
(d) C. R. Wade, A. E. J. Broomsgrove, S. Aldridge, F. P. Gabbaï, *Chem. Rev.* **2010**, *110*, 3958. doi:10.1021/CR900401A  
(e) *Functional Organic Materials* (Eds T. J. J. Müller, U. H. F. Bunz) **2007** (Wiley-VCH: Weinheim).  
(f) J. D. Tovar, *Acc. Chem. Res.* **2013**, *46*, in press. doi:10.1021/AR3002969  
(g) Y. N. Teo, E. T. Kool, *Chem. Rev.* **2012**, *112*, 4221. doi:10.1021/CR100351G
- [2] (a) F. Jäkle, *Chem. Rev.* **2010**, *110*, 3985. doi:10.1021/CR100026F  
(b) M. J. D. Bosdet, W. E. Piers, *Can. J. Chem.* **2009**, *87*, 8. doi:10.1139/V08-110  
(c) M. Elbing, G. C. Bazan, *Angew. Chem. Int. Ed.* **2008**, *47*, 834. doi:10.1002/ANIE.200703722  
(d) P. G. Campbell, A. J. V. Marwitz, S.-Y. Liu, *Angew. Chem. Int. Ed.* **2012**, *51*, 6074. doi:10.1002/ANIE.201200063
- [3] (a) T.-Y. Chu, J. Lu, S. Beaupré, Y. Zhang, J.-R. Pouliot, S. Wakim, J. Zhou, M. Leclerc, Z. Li, J. Ding, Y. Tao, *J. Am. Chem. Soc.* **2011**, *133*, 4250. doi:10.1021/JA200314M  
(b) J. Hou, H.-Y. Chen, S. Zhang, G. Li, Y. Yang, *J. Am. Chem. Soc.* **2008**, *130*, 16144. doi:10.1021/JA806687U  
(c) M. Shimizu, H. Tatsumi, K. Mochida, K. Oda, T. Hiyama, *Chem. – Asian J.* **2008**, *3*, 1238. doi:10.1002/ASIA.200800094
- [4] (a) T. Baumgartner, R. Réau, *Chem. Rev.* **2006**, *106*, 4681. doi:10.1021/CR040179M  
(b) J. Crassous, R. Réau, *Dalton Trans.* **2008**, 6865. doi:10.1039/B810976A  
(c) Y. Matano, H. Imahori, *Org. Biomol. Chem.* **2009**, *7*, 1258. doi:10.1039/B819255N  
(d) A. Fukazawa, S. Yamaguchi, *Chem. – Asian J.* **2009**, *4*, 1386. doi:10.1002/ASIA.200900179  
(e) Y. Ren, T. Baumgartner, *Dalton Trans.* **2012**, *41*, 7792. doi:10.1039/C2DT00024E
- [5] (a) T. Baumgartner, T. Neumann, B. Wirges, *Angew. Chem. Int. Ed.* **2004**, *43*, 6197. doi:10.1002/ANIE.200461301  
(b) T. Baumgartner, W. Bergmans, T. Kárpáti, T. Neumann, M. Nieger, L. Nyulász, *Chem. – Eur. J.* **2005**, *11*, 4687. doi:10.1002/CHEM.200500152  
(c) M. G. Hobbs, T. Baumgartner, *Eur. J. Inorg. Chem.* **2007**, 3611. doi:10.1002/EJIC.200700236  
(d) C. Romero-Nieto, T. Baumgartner, *Synlett* **2013**, *24*, 920. doi:10.1055/S-0032-1317804
- [6] Y. Ren, T. Baumgartner, *J. Am. Chem. Soc.* **2011**, *133*, 1328. doi:10.1021/JA108081B
- [7] Y. Ren, W. H. Kan, M. A. Henderson, P. G. Bomben, C. P. Berlinguette, V. Thangadurai, T. Baumgartner, *J. Am. Chem. Soc.* **2011**, *133*, 17014. doi:10.1021/JA206784F
- [8] Y. Ren, W. H. Kan, V. Thangadurai, T. Baumgartner, *Angew. Chem. Int. Ed.* **2012**, *51*, 3964. doi:10.1002/ANIE.201109205
- [9] Y. Ren, T. Baumgartner, *Inorg. Chem.* **2012**, *51*, 2669. doi:10.1021/IC2026335
- [10] H. Usta, G. Lu, A. Facchetti, T. J. Marks, *J. Am. Chem. Soc.* **2006**, *128*, 9034. doi:10.1021/JA062908G
- [11] Y. Dienes, S. Durben, T. Kárpáti, T. Neumann, U. Englert, L. Nyulász, T. Baumgartner, *Chem. – Eur. J.* **2007**, *13*, 7487. doi:10.1002/CHEM.200700399
- [12] Y. Dienes, M. Eggenstein, T. Neumann, U. Englert, T. Baumgartner, *Dalton Trans.* **2006**, 1424. doi:10.1039/B509277A
- [13] (a) F. Mathey, G. Müller, *Can. J. Chem.* **1978**, *56*, 2486. doi:10.1139/V78-406  
(b) S. Durben, Y. Dienes, T. Baumgartner, *Org. Lett.* **2006**, *8*, 5893. doi:10.1021/OL062580W
- [14] X. M. He, A. Y. Y. Woo, J. Borau-Gracia, T. Baumgartner, *Chem. – Eur. J.* **2013**, *19*, 7620. doi:10.1002/CHEM.201300052
- [15] M. J. Frisch, G. W. Trucks, H. B. Schlegel, G. E. Scuseria, M. A. Robb, J. R. Cheeseman, J. A. Jr, Montgomery, T. Vreven, K. N. Kudin, J. C. Burant, J. M. Millam, S. S. Iyengar, J. Tomasi, V. Barone, B. Mennucci, M. Cossi, G. Scalmani, N. Rega, G. A. Petersson, H. Nakatsuji, M. Hada, M. Ehara, K. Toyota, R. Fukuda, J. Hasegawa, M. Ishida, T. Nakajima, Y. Honda, O. Kitao, H. Nakai, M. Klene, X. Li, J. E. Knox, H. P. Hratchian, J. B. Cross, V. Bakken, C. Adamo, J. Jaramillo, R. Gomperts, R. E. Stratmann, O. Yazyev, A. J. Austin, R. Cammi, C. Pomelli, J. W. Ochterski, P. Y. Ayala, K. Morokuma, G. A. Voth, P. Salvador, J. J. Dannenberg, V. G. Zakrzewski, S. Dapprich, A. D. Daniels, M. C. Strain, O. Farkas, D. K. Malick, A. D. Rabuck, K. Raghavachari, J. B. Foresman, J. V. Ortiz, Q. Cui, A. G. Baboul, S. Clifford, J. Cioslowski, B. B. Stefanov, G. Liu, A. Liashenko, P. Piskorz, I. Komaromi, R. L. Martin, D. J. Fox, T. Keith, M. A. Al-Laham, C. Y. Peng, A. Nanayakkara, M. Challacombe, P. M. W. Gill, B. Johnson, W. Chen, M. W. Wong, C. Gonzalez, J. A. Pople, *Gaussian 03*, revision E.01; Gaussian Inc.: Wallingford, CT, **2007**.
- [16] *Bruker SAINT 2007* (Bruker AXS Inc.: Madison, WI).
- [17] G. M. Sheldrick, *Acta Crystallogr. A* **2008**, *64*, 112. doi:10.1107/S0108767307043930